# Frequency dependence of scaling exponents of hyperpolarizability in polyenes: A density-matrix renormalization-group approach

G. P. Zhang*
*Max-Planck-Institut für Physik komplexer Systeme, Nöthnitzer Strasse 38, D-01187 Dresden, Germany*
(Received 5 April 1999; revised manuscript received 14 June 1999)

Scaling properties of the second-order hyperpolarizability $\gamma$ in polyenes are investigated by the Lanczos-based density-matrix renormalization-group scheme. The numerical results suggest that the exponent $\eta$, characterizing the scaling law $\gamma/N \propto N^{\eta}$, is inversely proportional to the incident photon frequency $\omega$. The static exponent sets the maximum. The full relation can be cast into an analytical expression as $\eta(\omega)=b/(\omega+a)$, which allows one to directly compare the results measured at different frequencies and objectively evaluate the nonlinear optical performance of one specific material. The microscopic conditions for this relation are also discussed. [S0163-1829(99)01540-4]

## I. INTRODUCTION

One of the intriguing properties in the quasi-one-dimensional polymer chain is that the second-order optical hyperpolarizability $\gamma$ sharply increases with length $N$ as $\gamma/N \propto N^{\eta}$.[1] This greatly motivates many experimental[2–6] as well as theoretical investigations.[7–10] The exponent $\eta$ quantifies the increment of $\gamma$ per unit and naturally becomes the focus of many studies. Rigorously speaking, the above scaling law is only valid for a short chain. For a long chain, $\eta$ itself depends on chain length, and in particular saturates to 1 in the thermodynamical limit. Thus, the most meaningful range for $\eta$ is at length $N$ shorter than the saturation length. Theoretically, $\eta$ also depends on the model and parameters used. For a noninteracting model, it is found that $\chi^{(3)} \propto E_g^{-6}$,[11] where $E_g$ is the energy gap. In the interacting case, the situation is less obvious due to the complicated nature of electron correlation. Moreover, different from the thermodynamical properties, the scaling property of hyperpolarizability is rather elegant and should be calculated with a more sophisticated algorithm. One notices that the first attempt by the symmetrized density-matrix renormalization-group method (DMRG) failed to yield reliable results over $N=20$.[12] Nevertheless, generally one believes that $\eta$ ranges from 3 to 8. It should be noted that most of these exponents are calculated at zero frequency. Experimentally,[2–6] on the other hand, they are mostly measured at different nonzero frequencies.[13,14] In other words, they are not static. Thus there is no simple connection between the exponents experimentally measured and those theoretically calculated as the photon frequency may play a role here. As noted in various experiments,[14] this indeed becomes a big practical difficulty to objectively evaluate the nonlinear optical performance for one specific material. Our aim is to bridge this gap and build some quantitative relations.

The paper is arranged as follows. In Sec. II, we present the theoretical scheme and critically comment on the failure of the recent DMRG calculations. Section III is devoted to the results and discussions while the conclusion is presented in Sec. IV. In the Appendix, we explain the details of our numerical implementations.

## II. METHODOLOGY

We employ a combined version of the Lanczos iteration scheme and density-matrix renormalization-group (LDMRG) method[15,16] to investigate the frequency dependence of the scaling exponent of the second hyperpolarizabilities in polyenes. The numerical calculation was done up to $N=32$, where the scaling properties can be well fitted by the above scaling law. Our system is modeled by the one-dimensional dimerized extended-Hubbard model,[17]

$$\hat{H} = -t\sum_{i,\sigma}[1+(-1)^i\delta](c^{\dagger}_{i+1,\sigma}c_{i,\sigma}+\text{H.c.}) + U\sum_i n_{i\uparrow}n_{i\downarrow} + V\sum_i n_i n_{i+1}, \quad (1)$$

where $c^{\dagger}_{i,\sigma}$ ($c_{i,\sigma}$) is the electron creation (annihilation) operator with the spin orientation $\sigma(=\uparrow,\downarrow)$ at site $i$ and $n_{i,\sigma}=c^{\dagger}_{i,\sigma}c_{i,\sigma}$. Hereafter the on-site and intersite interactions $U$ and $V$ are in units of hopping integral $t$, and $t$ is chosen to be 1. Other parameters will be specified later. The half-filling case is considered. As before, we also use the current operator to form the starting vector $|f_i\rangle$. For the $A_g$ states, one constructs $|f_i\rangle$ by applying the current operator onto the ground state twice (for details, see the Appendix). 200 states of the density matrices are kept in each block with the truncation error below $10^{-9}$ and the relative error smaller than $10^{-2}$.[18]

Before we go further, it is worthwhile to make some critical comments on the performance of the standard DMRG scheme to calculate the dynamical properties as one already noticed its failure before. This helps to understand why the LDMRG can handle the nonlinear optical properties successfully. It is known that the usual DMRG is best suited for the ground-state calculations, while for the excited states it is not straightforward. A seeming reason is that these excited states lie high above the ground state and the truncation error is large, but actually as we found, this is not the major origin. The main problem is that one misses one's targets during DMRG iterations, or ''targeting catastrophe,'' while one cannot easily spot such missing in real calculations. Let us

 

analyze it in more detail. We know that in the ground-state calculations, one only needs to target the lowest-lying state and has no difficulty in identifying such a state. However, in the excited-state calculations, this becomes difficult since with an increase of chain length, quite often those desired excited states move out of and new states move into the original energy window. If one still sticks to one's original way of targeting states and does not preselect the states cautiously, one is very likely to target spurious or irrelevant states of different origins, which ultimately leads to the targeting catastrophe and the breakdown of calculations. To the best of our knowledge, such failure has never been carefully identified before, but it has already appeared in many of the recent DMRG calculations.[10,12] The typical symptom of such targeting catastrophe is that upon the increase of chain length, there is a sudden change of either eigenenergy, correlation length, or transition matrix elements. It has taken us quite a long time to figure out how to fix the problem effectively, but the answer turns out to be rather simple: *Filter out those irrelevant states beforehand and discriminatingly target states* (for a complete description, see the Appendix). This is the essence of the LDMRG scheme, which ensures that one will correctly target states by getting rid of numerous irrelevant states and avoiding the targeting catastrophe. Other technical details can be found in Ref. 15.

We use the formula from Ref. 19 to compute $\gamma$,

$$\begin{aligned}\gamma(-\omega_\sigma;\omega_1,\omega_2,\omega_3)=&K(-\omega_\sigma;\omega_1,\omega_2,\omega_3)(-\hbar)^{-3}I_{1,2,3}\\&\times\Bigg[\sum_{a,b,c}\Bigg(\frac{\mu_{ga}\mu_{ab}\mu_{bc}\mu_{cg}}{(\omega_a-\omega_\sigma)(\omega_b-\omega_1-\omega_2)(\omega_c-\omega_1)}+\frac{\mu_{ga}\mu_{ab}\mu_{bc}\mu_{cg}}{(\omega_a^*+\omega_3)(\omega_b-\omega_1-\omega_2)(\omega_c-\omega_1)}\\&+\frac{\mu_{ga}\mu_{ab}\mu_{bc}\mu_{cg}}{(\omega_a^*+\omega_1)(\omega_b^*+\omega_1+\omega_2)(\omega_c-\omega_3)}+\frac{\mu_{ga}\mu_{ab}\mu_{bc}\mu_{cg}}{(\omega_a^*+\omega_1)(\omega_b^*+\omega_1+\omega_2)(\omega_c^*+\omega_\sigma)}\Bigg)\\&-\sum_{a,c}\Bigg(\frac{\mu_{ga}\mu_{ag}\mu_{gc}\mu_{cg}}{(\omega_a-\omega_\sigma)(\omega_a-\omega_3)(\omega_c-\omega_1)}+\frac{\mu_{ga}\mu_{ag}\mu_{gc}\mu_{cg}}{(\omega_a-\omega_3)(\omega_c^*+\omega_2)(\omega_c-\omega_1)}\\&+\frac{\mu_{ga}\mu_{ag}\mu_{gc}\mu_{cg}}{(\omega_a^*+\omega_\sigma)(\omega_a^*+\omega_3)(\omega_c^*+\omega_1)}+\frac{\mu_{ga}\mu_{ag}\mu_{gc}\mu_{cg}}{(\omega_a^*+\omega_3)(\omega_c-\omega_2)(\omega_c^*+\omega_1)}\Bigg)\Bigg],\end{aligned}\tag{2}$$

where $g$ refers to the ground state; $a$ and $c$ denote $B_u$ states; $b$ represents $A_g$ states; $\mu_{ij}$ is the transition matrix element between states $i$ and $j$. $\omega_\sigma=\omega_1+\omega_2+\omega_3$. $K(-\omega_\sigma;\omega_1,\omega_2,\omega_3)$ is a constant which depends on the incident photon frequencies $\omega_1,\omega_2,\omega_3$.[19] $I_{1,2,3}$ represents the permutation over $\omega_1,\omega_2,\omega_3$. $\hbar$ is the Planck constant over $2\pi$.

## III. RESULTS AND DISCUSSIONS

Quite different from many other techniques, such as the correction vector method,[20] the LDMRG algorithm enables us to calculate the optical responses over the entire frequency range, i.e., both at zero and nonzero frequencies, without repeating the same procedure for each frequency explicitly. This saves not only CPU time but also the computer memory space. To have some flavor of the dispersion of $\gamma$, in Fig. 1 we plot the third-harmonic generations $|\gamma(-3\omega)|[\equiv|\gamma(-3\omega;\omega,\omega,\omega)|]$ for four different chain lengths. Here we take $U=2$ and $V=0.8$. For convenience, hereafter, the amplitudes of $|\gamma|$ are in the same but arbitrary units, so they are comparable throughout the different figures. The frequency $\omega$ is also in units of $t$. In Fig. 1(a), the length $N$ is 10. One can see three clear peaks in the spectrum, where we introduce a small damping of 0.05 $t$. The first peak is at $\omega=0.318$, corresponding to the three-photon absorption due to the $1B_u$. The second (also largest) peak appears at $\omega=0.755$, which corresponds to the transition $|\Psi_{gs}\rangle\rightarrow|\Psi_{1B_u}\rangle\rightarrow|\Psi_{2A_g}\rangle\rightarrow|\Psi_{1B_u}\rangle\rightarrow|\Psi_{gs}\rangle$. Its intensity is about three times that of the first peak. Another small peak is at the right-hand shoulder of the main peak. Different from the first peak, it can be shown that this peak results from the finite-size effect. In the long chain limit, it will disappear. As we increase the length to $N=12$, this peak really goes away [see Fig. 1(b)]. Compared with Fig. 1(a), both the first and second peaks are redshifted. This is due to the fact that the charge becomes more delocalized as the length increases. It is no-

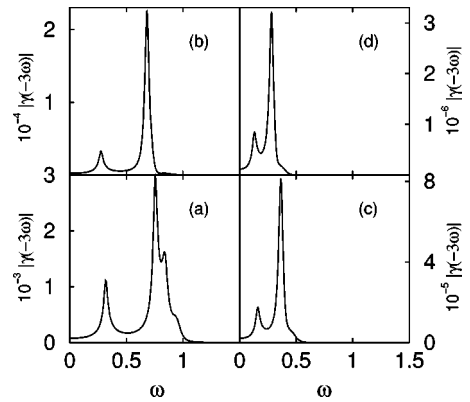


FIG. 1. Dispersion of the second-order hyperpolarizability. As the chain length increases, the peaks' positions redshift and the intensities enhance sharply. Here $U=2$ and $V=0.8$.

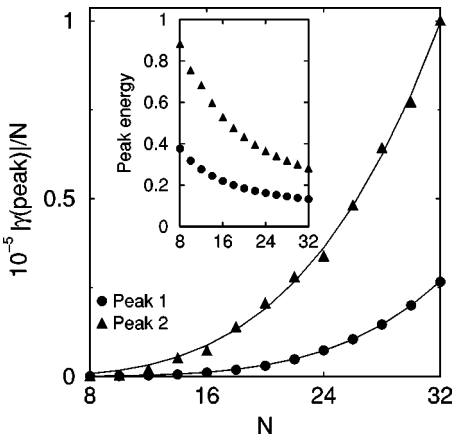


FIG. 2. The intensities and positions of two peaks in Fig. 1 change with chain length. The scaling behavior of $\gamma$ exhibits the frequency dependence.

ticeable that a significant enhancement of intensity with length is achieved. Further increasing the length to $N=24$ [see Fig. 1(c)], we find that the intensity contrast between these two peaks becomes larger than that at $N=10$. Besides a similar redshift of two main peaks, they move closer, but do not overlap even if we increase the chain length up to $N=32$ [see Fig. 1(d)].

To have a clear view, in Fig. 2 we illustrate both the peak energy (inset) and the peak intensity as a function of $N$. The filled circles refer to peak 1 (the smaller one) while the filled up-triangles refer to peak 2 (the larger one). As expected, both peak energies decrease with the increase of length $N$ (redshifting). The smaller peak converges more slowly than the larger one. The gap between these two peaks is 0.15 at $N=32$. From Fig. 2, one sees more clearly that both intensities $|\gamma(-3\omega;\omega,\omega,\omega)|/N$ increase sharply upon the increase of chain length. A fit of these intensities to the power law, $N^{\eta}$, is shown in solid lines, where we find $\eta=4.6$ is for peak 1 while 3.5 for peak 2. This means that the increment of the intensity of the smaller peak is faster than that of the larger one although the absolute value of the small peak is much smaller. To our knowledge, this is the first evidence that the exponent depends on the photon frequency: a larger $\eta$ corresponds to a smaller frequency.

Up to now, to the best of our knowledge, there have been very few theoretical investigations addressing the frequency-dependent exponent, especially in the interacting case, though many experiments call for it.[2–6,13,14] Understandably, to calculate these exponents accurately is still a big challenge to theory, in particular with the presence of the electron correlation. It is advantageous that we are able to do it quantitatively and comfortably within the LDMRG scheme. As already noted above, we do see evidence of the frequency dependence of the exponent. The same thing is true for the static scaling dependence of $|\gamma(0)|/[\equiv|\gamma(0;0,0,0)|]$. For $U=2$, the results are displayed in Fig. 3(a). A polynomial fitting to the static scaling dependence of $\gamma$ on $N$ shows that $|\gamma(0)|$ scales as $|\gamma(0)|/N\propto N^{5.1}$. This static exponent is larger than the dynamical exponents of both peaks 1 and 2, which means the same thing: a smaller frequency leads to a larger $\eta$. For other parameters, such as $U=3$, $V=1.2$ [with the static results shown in Fig. 3(b)], we also observe a similar dependence of $\eta$ on frequency.

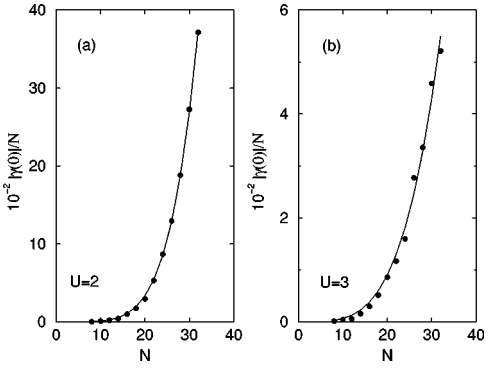


FIG. 3. The static hyperpolarizability increases more sharply than that of nonzero frequencies for both $U=2$ and 3. This demonstrates a similar tendency as shown in Fig. 2.

We would like to verify whether this represents a generic feature or not. In order to do so, we performed extensive calculations for different parameters, both with and without dimerizations, which represent a wide range of conjugated polyenes and hopefully cover other linear chains as well. The results are shown in Fig. 4. The used parameters[21] are given in the following order: $[U, V, \delta]$: (0) [3.0, 1.2, 0.07]; (1) [3.0, 1.2, 0.0]; (2) [3.0, 1.8, 0.07]; (3) [1.0, 0.4, 0.0]; (4) [3.0, 1.5, 0.0]; (5) [5.0, 3.0, 0.2]; (6) [3.0, 1.8, 0.0]; (7) [3.0, 0.6, 0.0]; (8) [3.0, 1.5, 0.04]; (9) [4.0, 2.4, 0.1]; ($\times$) [2.0, 0.8, 0.0]; ($\otimes$) [4.0, 2.4, 0.2]. To have an easy view, we normalize the photon frequency with respect to their maximal peak frequencies. The figure shows that for different parameters, the dependence of $\eta$ on $\omega$ changes a lot, but all exhibit a common tendency: *$\eta$ is inversely proportional to the incident photon frequency*. Interestingly, our finding is also supported by the previous *ab initio* results[22] (see the inset in Fig. 4). One notices a similar decrease of the exponent with the photon frequency. The full relation can be cast into an analytical expression,

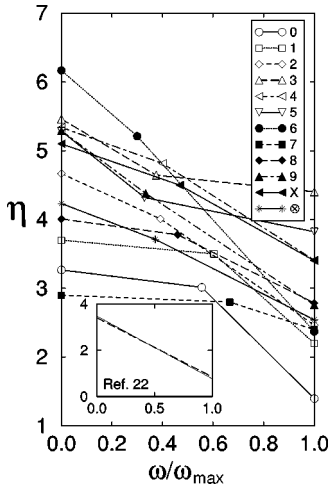


FIG. 4. An extensive numerical justification for the frequency-dependence relation of the exponent $\eta$. Note the photon frequencies $\omega$ are normalized to their respective maximal frequencies $\omega_{\max}$. The used parameters are given in the following order: $[U, V, \delta]$: (0) [3.0, 1.2, 0.07]; (1) [3.0, 1.2, 0.0]; (2) [3.0, 1.8, 0.07]; (3) [1.0, 0.4, 0.0]; (4) [3.0, 1.5, 0.0]; (5) [5.0, 3.0, 0.2]; (6) [3.0, 1.8, 0.0]; (7) [3.0, 0.6, 0.0]; (8) [3.0, 1.5, 0.04]; (9) [4.0, 2.4, 0.1]; ($\times$) [2.0, 0.8, 0.0]; ($\otimes$) [4.0, 2.4, 0.2]. Inset: the data are from Ref. 22.

$$\eta(\omega)=\frac{b}{\omega+a}, \tag{3}$$

where $a$ and $b$ are material-specific constants; $\omega$ is the incident photon frequency. The physical meanings of $a$ and $b$ are that the ratio $b/a$ represents the static exponent and $a$ describes how quickly the photon frequency affects the exponent. For $U=2$, $V=0.8$, we find that $a=0.12$ and $b=0.61$. Experimentally, Puccetti *et al.* obtained $\eta=4.65$ at 1.34 $\mu$m for their series I with *bis*-donor substitution at the end.[14] If they can measure another point, one can extract two constants and eventually extrapolate the static exponent.

We believe that such analytical expression is useful to experimentalists. As known, many measurements, especially these earlier ones, were mostly performed at one or two wavelengths, such as 532 and 1064 nm. It is hard to judge whether they give an objective evaluation of one material. Quite often, one chooses material by looking for those exhibiting large $\gamma$.[6] Unfortunately, such selection neither necessarily ensures a large enhancement of the $\gamma$ with chain length, nor rules out the frequency effect. Thus theory indeed can play an active role here. The above analytical formula provides a simple way to make a direct comparison among exponents measured at different frequencies and rationalizes their differences.[13] Since the present results are obtained with explicitly taking into account the electron interaction, the conclusion should be quite general, at least for those low-dimensional systems.

Finally, it is also equally important to investigate the microscopic conditions for the above relation. We found that within all our tested cases, for the well-defined peaks, the exponents obey the above relationship very well, but for those ill-defined ones they may behave differently. Here we give an example. For $U=3$ and $V/U=0.4$, $\delta=0.07$, at $N=8$, a peak is located at $\omega=1.2$. Its intensity increases with chain length up to $N=22$ and then decreases. Thus, in this case, even the usual scaling law does not work. This is a consequence of the finite-size effect. The chain-length dependence of hyperpolarizabilities for those ill-defined peaks hardly fits into any simple picture. Fortunately, these peaks are of little interest in practice since their susceptibilities are usually too small. Nevertheless, one should be cautious to apply the above relation to those ill-defined peaks.

## IV. CONCLUSIONS

In conclusion, we have explored the scaling properties of the second-order optical hyperpolarizability $\gamma$ by the Lanczos-based DMRG method for the finite polyenes. Our results suggest that there is a clear dependence of the scaling exponent $\eta$ on the incident photon frequency $\omega$: $\eta$ becomes smaller as $\omega$ increases. The static exponent is the maximum which one can get for one specific material. The relation can be concisely cast into an analytical expression, $\eta(\omega)=b/(\omega+a)$. This builds up a simple connection between the static and dynamic exponents, which gives a way to have an objective comparison among the experimentally measured scaling exponents. Since our results are obtained within an interacting model Hamiltonian, the conclusion should be generic, at least for low-dimensional systems of our interest. Finally, we discuss the microscopic conditions of the relation.

## ACKNOWLEDGMENTS

The author would like to acknowledge support from the Max-Planck-Institut für Physik komplex Systeme, in Dresden, Germany, where the main part of work was done.

## APPENDIX

In this appendix, we give some additional details of our LDMRG scheme, which are very critical to calculate the dynamical properties. The main point is to effectively target states. We recommend two different ways of targeting states.

(i) For the one-photon states, one can use $\Phi=J|\Psi_{gs}\rangle$ to form the density matrix $\rho_{ii'}=\Sigma_j\Phi_{ij}\Phi_{i'j}$ (after normalizing $\Phi$). $J$ is the current operator.[15] Here one implicitly includes the weights for all the desired states since the weight itself is the amplitude of the transition matrix element. The beauty of such targeting is that one surely targets only dipole-allowed states because other states contribute a zero weight. This helps one to avoid the targeting catastrophe. For the two-photon or three-photon states, one uses $\Phi=J^2|\Psi_{gs}\rangle$ or $J^3|\Psi_{gs}\rangle$ to form density matrices. Analogously, we can circumvent the targeting catastrophe. If all these states are desired, then the whole density matrix is simply a summation over them. Note that in any case the ground state must be targeted.

(ii) Explicitly targeting states. One uses all the explicit eigenstates $\{\Psi_\nu\}$ to form density matrices, such as $\rho_{ii'}=\Sigma_{\nu,j}w_\nu\Psi_\nu^{ij}\Psi_\nu^{i'j}$. The weights $w_\nu$ can be the same for all the states or slightly larger for most significant states. This scheme requires that one explicitly calculates eigenstates $\{\Psi_\nu\}$. Through the LDMRG, we are sure that these states must be our desired states. In addition, we strongly suggest that besides the usual Lanczos and Davidson schemes, one should consider using the asymmetrical shifting diagonal elements (ASDE) method. We find that the ASDE is much superior to the traditional scheme, in particular when the absolute values of diagonal elements are very large.

Finally, let us make some remarks on these two schemes. Our experience shows that scheme (i) usually gives an overall good shape of the spectrum while scheme (ii) gives a most accurate result for a few particular states or peaks. Thus depending on one's specific requirements, one may choose (i) or (ii) or combine (i) and (ii).

*Present address: Max-Planck-Institut für Mikrostrukturphysik, Weinberg 2, D-06120 Halle, Germany. Electronic address: zhang@mpi-halle.mpg.de

[1] J. P. Herrmann and J. Ducuing, J. Appl. Phys. **45**, 510 (1974); J. R. Heflin *et al.*, Phys. Rev. B **38**, 1573 (1988).

[2] D. S. Chemla and J. Zyss, *Nonlinear Optical Properties of Organic Molecules and Crystals* (Academic, New York, 1986).

[3] I. D. W. Samuel *et al.*, Science **265**, 1070 (1994).

[4] A. Mathy *et al.*, Phys. Rev. B **53**, 4367 (1996).
[5] G. S. W. Graig *et al.*, Macromolecules **27**, 1875 (1994).
[6] S. R. Marder *et al.*, Science **261**, 186 (1993); **263**, 511 (1994); **265**, 632 (1994); **276**, 1233 (1997).
[7] D. Beljonne, Z. Shuai, and J. L. Bredas, J. Chem. Phys. **98**, 8819 (1993).
[8] B. M. Pierce, J. Chem. Phys. **91**, 791 (1989).
[9] F. S. Spano and Z. G. Soos, J. Chem. Phys. **99**, 9265 (1993).
[10] W. Barford, R. J. Bursill, and M. Y. Lavrentiev, J. Phys.: Condens. Matter **10**, 6429 (1998); M. Boman and R. J. Bursill, Phys. Rev. B **57**, 15 167 (1998).
[11] G. P. Agrawal, C. Cojan, and C. Flytzanis, Phys. Rev. B **17**, 776 (1978); K. C. Rustagi and J. Ducuing, Opt. Commun. **10**, 258 (1974).
[12] Z. Shuai, J. L. Bredas, A. Saxena, and A. R. Bishop, J. Chem. Phys. **109**, 2549 (1998); Z. Shuai, J. L. Bredas, S. K. Pati, and S. Ramasesha, Phys. Rev. B **58**, 15 329 (1998).
[13] C. Bubeck, *Electronic Materials: The Oligomer Approach*, edited by K. Müllen and G. Wegner (Wiley-VCH, Berlin, 1998), Chap. 8.
[14] See, for example, M. Blanchard-Desce, J.-M. Lehn, M. Barzoukas, C. Runser, A. Ford, G. Puccetti, I. Ledoux, and J. Zyss, Nonlinear Opt. **10**, 23 (1995); G. Puccetti, M. Blanchard-Desce, I. Ledoux, J.-M. Lehn, and J. Zyss, J. Phys. Chem. **97**, 9385 (1993).
[15] G. P. Zhang, T. F. George, and L. N. Pandey, J. Chem. Phys. **109**, 2562 (1998); G. P. Zhang and X. F. Zong, Chem. Phys. Lett. **308**, 289 (1999).
[16] G. P. Zhang, Comput. Phys. Commun. **109**, 27 (1998).
[17] G. P. Zhang, Phys. Rev. B **56**, 9189 (1997).
[18] We estimated it (a) at $U=V=0$ and (b) by keeping a different number of states of density matrices. The experimental error is never smaller than this.
[19] B. J. Orr and J. F. Ward, Mol. Phys. **20**, 513 (1971).
[20] Z. G. Soos and S. Ramasesha, J. Chem. Phys. **90**, 1067 (1989).
[21] We have more data than those presented, but all exhibit a similar trend. For clarity, some of them are shown here.
[22] Y. Luo, H. Agren, H. Koch, P. Jorgensen, and T. Helgaker, Phys. Rev. B **51**, 14 949 (1995).